NFN - Nationales Forschungsnetzwerk

Geometry + Simulation

http://www.gs.jku.at

# Spectral analysis of geometric multigrid methods for isogeometric analysis

C. Hofreither, W. Zulehner

G+S Report No. 24

December 2014

Der Wissenschaftsfonds.

JOHANNES KEPLER UNIVERSITY LINZ

# Spectral analysis of geometric multigrid methods for isogeometric analysis

Clemens Hofreither[1] and Walter Zulehner[1]

Institute of Computational Mathematics,
Johannes Kepler University Linz,
Altenbergerstr. 69, 4040 Linz, Austria

**Abstract.** We investigate geometric multigrid methods for solving the large, sparse linear systems which arise in isogeometric discretizations of elliptic partial differential equations. We observe that the performance of standard V-cycle iteration is highly dependent on the spatial dimension as well as the spline degree of the discretization space. Conjugate gradient iteration preconditioned with one V-cycle mitigates this dependence, but does not eliminate it. We perform both classical local Fourier analysis as well as a numerical spectral analysis of the two-grid method to gain better understanding of the underlying problems and observe that classical smoothers do not perform well in the isogeometric setting.

## 1 Introduction

Isogeometric analysis (IGA), a numerical technique for the solution of partial differential equations first proposed in [7], has attracted considerable research attention in recent years. The efficient solution of the discretized systems arising in isogeometric analysis has been the topic of several publications [3,8,4,5,2,6]. In the present paper, our interest lies in geometric multigrid methods for isogeometric analysis. Our aim in this article is mainly to enhance the understanding of multigrid methods for IGA by spectral analysis and more extensive numerical experiments. In particular, we are interested in the effect the spline degree has on the performance of multigrid iteration. The experiments from [6] show that, while convergence rates for standard V-cycle iteration are $h$-independent as predicted by the theory, they depend strongly on the spline degree $p$. This effect is more pronounced in higher space dimensions. We investigate this effect in more detail by analyzing the performance of classical smoothers as well as of the coarse-grid correction step for different space dimensions and spline degrees. We also clarify to what extent boundary effects are responsible.

We outline a simple geometric multigrid solver for IGA. After performing some basic iteration number tests both with pure V-cycle iteration and with CG iteration preconditioned by a V-cycle, we perform local Fourier analysis in 1D. We then perform a more detailed numerical spectral analysis of the smoother and the coarse-grid correction step for the eigenfunctions of the discretized problem in order to elucidate the effect that increasing the spline degree has.

## 2 Geometric multigrid for isogeometric analysis

For space reasons, we cannot present a full IGA framework and instead consider a simple model problem. See, e.g., [7] for more details. Let $\mathcal{V}_h \subset H_0^1(\Omega)$ denote a tensor product B-spline space over $\Omega = [0,1]^d$. We consider an IGA discretization of the Poisson equation with pure Dirichlet boundary conditions: find $u_h \in \mathcal{V}_h$ such that

$$a(u_h, v_h) = \langle F, v_h \rangle \qquad \forall v_h \in \mathcal{V}_h$$

with the bilinear form and linear functions, respectively,

$$a(u,v) = \int_\Omega \nabla u \cdot \nabla v \, dx, \qquad \langle F, v \rangle = \int_\Omega f v \, dx - a(\tilde{g}, v).$$

Here $\tilde{g} \in H^1(\Omega)$ is a suitable extension of the given Dirichlet data.

In the following, we outline the construction of a simple geometric multigrid scheme for this problem. Let $\mathcal{V}_0$ denote a coarse tensor product spline space over $(0,1)^d$. Performing uniform and global $h$-refinement by knot insertion, we obtain a sequence of refined spline spaces $\mathcal{V}_1, \mathcal{V}_2, \dots$ Let $\mathcal{V}_H$ and $\mathcal{V}_h$ denote two successive spline spaces in this sequence, and let $P : \mathcal{V}_H \to \mathcal{V}_h$ denote the prolongation operator from the coarse to the fine space. One step of the two-grid iteration process is given by a pre-smoothing step, the coarse-grid correction, and a post-smoothing step; i.e., given $u_0 \in \mathcal{V}_h$, the next iterate $u_1$ is obtained by

$$\begin{aligned} u^{(1)} &:= u_0 + S^{-1}(f_h - A_h u_0), \\ u^{(2)} &:= u^{(1)} + P A_H^{-1} P^\top (f_h - A_h u^{(1)}), \\ u_1 := u^{(3)} &:= u^{(2)} + S^{-\top}(f_h - A_h u^{(2)}). \end{aligned}$$

Here, $S$ is a suitable smoother for the fine-space stiffness matrix $A_h$.

As usual, a multigrid scheme is obtained by considering a hierarchy of nested spline spaces and replacing the exact inverse $A_H^{-1}$ in the above procedure recursively with the same procedure applied on the next coarser space, until $\mathcal{V}_0$ is reached. We consider only the case of a single coarse-grid correction step, i.e., the V-cycle.

To test the multigrid iteration, we set up the Poisson equation $-\Delta u = f$ with pure Dirichlet boundary conditions on $\Omega = (0,1)^d$. We choose tensor product B-spline basis functions defined on equidistant knot vectors with spline degrees $p$ in every direction and maximum continuity, i.e., simple interior knots. The right-hand side $f$ and the boundary conditions are chosen according to the exact solution $u(x) = \prod_{i=1}^d \sin(\pi(x_i + 0.5))$.

We then choose a random starting vector and perform V-cycle iteration as described above. In Table 1, left half, we display the iteration numbers required to reduce the initial residual by a factor of $10^{-8}$ in the Euclidean norm. The $h$-independence is clearly observed. Furthermore, the scheme is highly efficient for low spline degree $p$, yielding very low iteration numbers. In higher dimensions, in particular for $d = 3$, we see a dramatic increase in the number of iterations as the spline degree is increased. Very similar results have been observed in [6].

| | | V-cycle iteration | | | | PCG iteration | | | |
|---|---|---|---|---|---|---|---|---|---|
| $d$ | $N$ | $p$ | | | | $p$ | | | |
| | | 1 | 2 | 3 | 4 | 1 | 2 | 3 | 4 |
| 1 | ∼4,1k | 11 | 8 | 7 | 9 | 7 | 6 | 5 | 6 |
| | ∼262k | 11 | 8 | 7 | 9 | 7 | 5 | 5 | 6 |
| 2 | ∼66k | 9 | 11 | 37 | 127 | 6 | 7 | 14 | 27 |
| | ∼1,05m | 9 | 11 | 36 | 125 | 6 | 7 | 14 | 27 |
| 3 | ∼40k | 9 | 38 | 240 | 1682 | 6 | 15 | 37 | 100 |
| | ∼290k | 9 | 38 | 236 | 1564 | 6 | 15 | 37 | 98 |

**Table 1.** V-cycle iteration numbers for the model Poisson problem. Columns from left to right: space dimension $d$, number of unknowns $N$, V-cycle iteration numbers for $p = 1$ to 4, iteration numbers for CG preconditioned with V-cycle for $p = 1$ to 4.

We also test preconditioned conjugate gradient (PCG) iteration with one V-cycle as the preconditioner; see Table 1, right half. The iteration numbers are significantly reduced for the previously unsatisfactory cases with $d = 3$ and high spline degree $p$. A clear dependence of the iteration numbers on $d$ and $p$ remains.

We remark that the results remain quantitatively very similar for the model problem $-\Delta u + u = f$ with pure Neumann boundary conditions.

## 3 Local Fourier analysis

We perform local Fourier analysis (LFA) for the two-grid method in the case $d = 1$ as described in the literature [9,1]. For this, we set up a space of B-splines of degree $p$ on $\mathbb{R}$ with uniformly spaced knots $\mathbb{Z} \cdot h$ at distances $h = 1$ as well as the corresponding nested coarse space with knots at $\mathbb{Z} \cdot H$, $H = 2h$. We then compute, for $p$ from 1 to 4, the stencils of the variational form of the operator $-\partial_{xx}$ on the fine space,

$$h^{-1}(-1, 2, -1),$$
$$h^{-1}(-\tfrac{1}{6}, -\tfrac{1}{3}, 1, -\tfrac{1}{3}, -\tfrac{1}{6}),$$
$$h^{-1}(-\tfrac{1}{120}, -\tfrac{1}{5}, -\tfrac{1}{8}, \tfrac{2}{3}, -\tfrac{1}{8}, -\tfrac{1}{5}, -\tfrac{1}{120}),$$
$$h^{-1}(-\tfrac{1}{5040}, -\tfrac{59}{2520}, -\tfrac{17}{90}, -\tfrac{11}{360}, \tfrac{35}{72}, -\tfrac{11}{360}, -\tfrac{17}{90}, -\tfrac{59}{2520}, -\tfrac{1}{5040}),$$

and the stencils of the canonical embedding of the coarse in the fine space,

$$(\tfrac{1}{2}, 1, \tfrac{1}{2})^\top, (\tfrac{1}{4}, \tfrac{3}{4}, \tfrac{3}{4}, \tfrac{1}{4})^\top, (\tfrac{1}{8}, \tfrac{1}{2}, \tfrac{3}{4}, \tfrac{1}{2}, \tfrac{1}{8})^\top, (\tfrac{1}{16}, \tfrac{5}{16}, \tfrac{5}{8}, \tfrac{5}{8}, \tfrac{5}{16}, \tfrac{1}{16})^\top.$$

We study the effect of these stencils on the Fourier modes $(\exp(\mathrm{i}\alpha\theta))_{\alpha\in\mathbb{Z}}$ for $\theta \in (-\pi, \pi)$. As usual, the analysis decomposes into two parts, namely the low frequencies $|\theta| < \pi/2$ and the high frequencies $|\theta| \geq \pi/2$. Following the standard procedure, we can compute the symbols of the fine-grid and prolongation operators $\hat{A}_h(\theta) \in \mathbb{C}^{2\times 2}$, $\hat{P}(\theta) \in \mathbb{C}^{2\times 1}$, respectively, based on the stencils above, as well as the derived symbols $\hat{R}(\theta) = \hat{P}(\theta)^* \in \mathbb{C}^{1\times 2}$, $\hat{A}_H(\theta) =$

$\hat{R}(\theta)\hat{A}_h(\theta)\hat{P}(\theta) \in \mathbb{C}^{1\times 1}$ of the restriction and coarse-grid operators, respectively. Due to the use of Galerkin projection for constructing the coarse-grid operator, we have $\hat{R}(\theta) = (\hat{P}(\theta))^*$. For simplicity we analyze here only the Richardson smoother, $S = \tau^{-1}I$, so that we have $\hat{G}_S(\tau,\theta) = I - \tau\hat{A}_h(\theta) \in \mathbb{C}^{2\times 2}$ for the symbol of the error reduction operator $G_S = I - S^{-1}A_h$. The error reduction rate of the two-grid operator is given by the spectral radius of

$$\widehat{\mathcal{TG}}(\tau,\theta) = \hat{G}_S(\tau,\theta)^* \left(I - \hat{P}(\theta)\hat{A}_H(\theta)^{-1}\hat{R}(\theta)\hat{A}_h(\theta)\right)\hat{G}_S(\tau,\theta) \in \mathbb{C}^{2\times 2}.$$

For fixed $\tau$, we approximate the maximum $\max_{\theta\in(-\pi,\pi)} \sigma(\widehat{\mathcal{TG}}(\tau,\theta))$ by sampling $\theta$ at equidistant points. The resulting error reduction rates are shown as functions of $\tau$ in Figure 1 for the cases $p = 1, 2, 3, 4$. Furthermore, the experimentally determined optimal choice of $\tau$ together with resulting error reduction factor $1/\sigma(\widehat{\mathcal{TG}}(\tau,\theta))$ is shown in Table 2, left column. We compare these results with the rates obtained in practice for a boundary value problem on $(0, 1)$, set up to have zero solution. The error reduction factor is here computed as the maximum ratio between the Euclidean norms of two successive iterates in the two-grid iteration, i.e., the worst-case error reduction. These numbers are shown in Table 2, middle column. The optimal choice for $\tau$ was found experimentally.

We observe that the numbers begin to deviate significantly from the theoretical LFA results as $p$ is increased. This is due to the influence of the boundary conditions, which are neglected in the LFA. The theoretical rates can be approached by performing extra smoothing near the boundaries. As suggested in [1], we use Kaczmarz iteration for this purpose. In our tests, 5 Kaczmarz sweeps on the first and last equations in the linear system, performed before the presmoothing step, were sufficient to approach the theoretical rates quite closely, as shown in Table 2, right column.

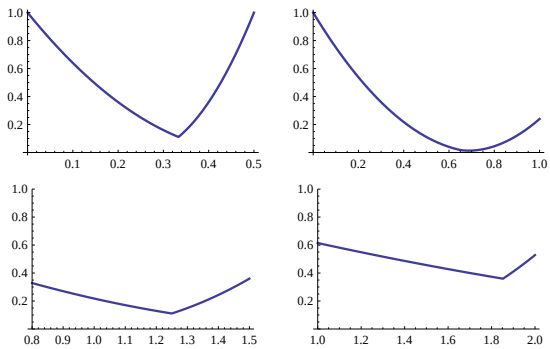


**Fig. 1.** Error reduction rates in dependence of $\tau$ ($x$-axis) computed by LFA in 1D with $p = 1, 2$ (top), $p = 3, 4$ (bottom).

| | Local Fourier analyis | | numerical results | | with boundary sweeps | |
|---|---|---|---|---|---|---|
| $p$ | $\tau_{\text{opt}}$ | error reduc. | $\tau_{\text{opt}}$ | error reduc. | $\tau_{\text{opt}}$ | error reduc. |
| 1 | 0.33 | 9.00 | 0.33 | 8.82 | 0.33 | 9.01 |
| 2 | 0.69 | 75.50 | 0.69 | 74.10 | 0.69 | 74.20 |
| 3 | 1.25 | 9.00 | 1.04 | 4.94 | 1.25 | 9.09 |
| 4 | 1.85 | 2.78 | 1.25 | 1.81 | 1.85 | 2.83 |

**Table 2.** Results of LFA for the 1-D case and comparison to numerical results.

We conclude that the results of the LFA are a good predictor for the performance of the multigrid method, in particular if additional smoothing is performed near the boundaries. Without these boundary sweeps, the performance of the method suffers, but this is not the main factor in the bad performance of the multigrid method: even in the boundary-less case of the LFA, the rates deteriorate as $p$ is increased.

## 4 Numerical spectral analysis

In this section, we take an alternative approach to spectral analysis which operates directly on the matrices used in the multigrid method and can therefore capture boundary effects.

We consider the problem $\Delta u = 0, u|_{\partial\Omega} = 0$ with $u = 0$ as its exact solution, and set up a two-grid scheme as above with $N$ unknowns on the fine grid. For a given vector $\mu \in \mathbb{R}^d$, we perform one step of the symmetrized Gauss-Seidel smoother, or one coarse-grid correction step, and measure the Euclidean norm of the result. That is, we compute the error reduction factors

$$r^{\text{S}}(\mu) = \frac{|G_{S^\top} G_S \mu|}{|\mu|}, \quad r^{\text{CGC}}(\mu) = \frac{\left|(I - P A_H^{-1} P^\top A_h)\mu\right|}{|\mu|}.$$

As a basis, we choose the generalized eigensystem $(\mu_j)$ which satisfies

$$A_h \mu_j = \lambda_j M_h \mu_j, \qquad j = 1, \dots, N,$$

where $M_h$ is the mass matrix of the fine-grid isogeometric basis. In Figures 2-4, we analyze the 1D, 2D, and 3D Laplace problem, respectively, using the Gauss-Seidel smoother. Each figure contains one plot each for spline degrees $p = 1, 2, 3, 4$. In each plot, we display the error reduction factors $r^{\text{S}}(\mu_j)$ and $r^{\text{CGC}}(\mu_j)$ for the generalized eigenvectors over their respective eigenvalues $\lambda_j$. The studied problems were relatively small, up to around $N = 1000$.

Throughout, the coarse-grid correction step reduces the lower part of the spectrum in an efficient manner. The Gauss-Seidel smoother however fails to perform robustly as the spline degree $p$ is increased. Already in 1D, the plot for $p = 4$ suggests difficulties for higher spline degrees. These difficulties start earlier for higher space dimensions, as we see from the plots for $d = 2, p = 4$ as well

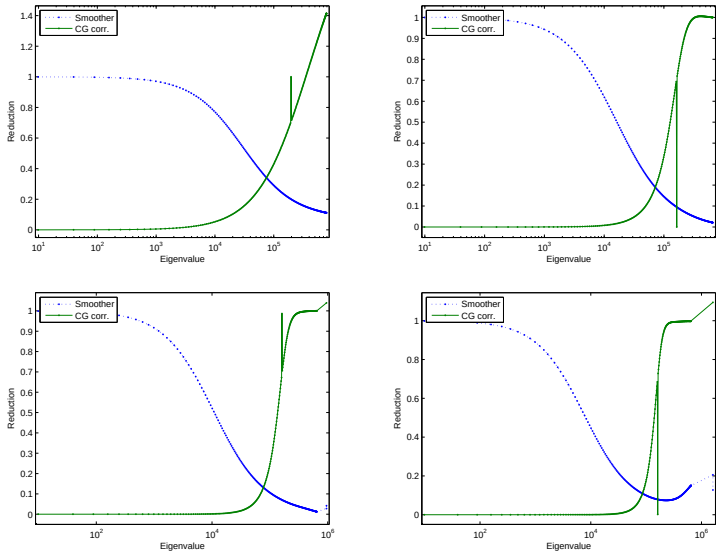


**Fig. 2.** Error reduction in the basis $(\mu_j)$ in 1D with $p = 1, 2$ (top), $p = 3, 4$ (bottom).

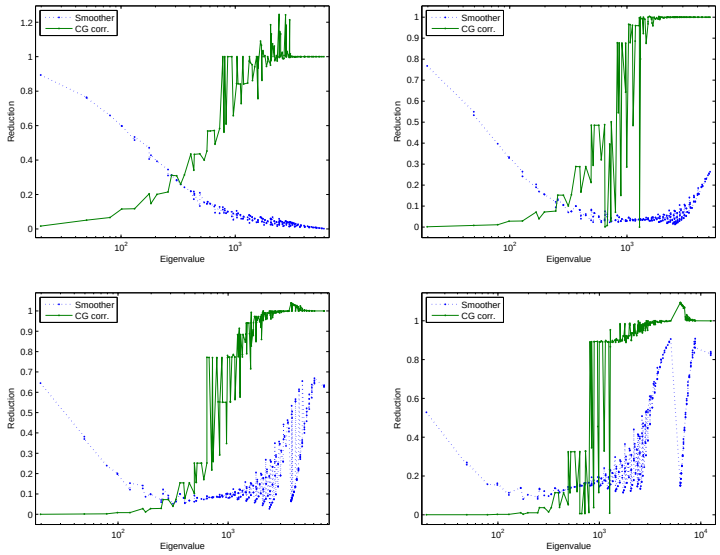


**Fig. 3.** Error reduction in the basis $(\mu_j)$ in 2D with $p = 1, 2$ (top), $p = 3, 4$ (bottom).

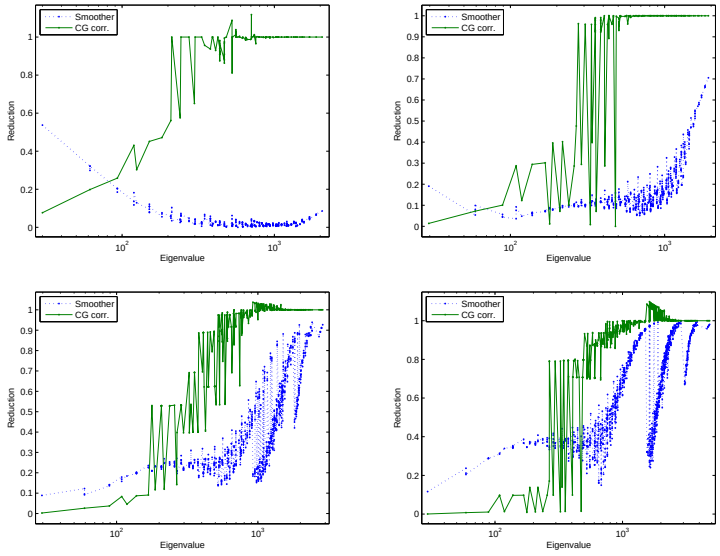


**Fig. 4.** Error reduction in the basis $(\mu_j)$ in 3D with $p = 1, 2$ (top), $p = 3, 4$ (bottom).

as $d = 3, p = 3$. Here the smoother starts to become unusable, reducing some high-frequency components by 10% or less.

We also test the damped Jacobi smoother, $S^{-1} = \tau \operatorname{diag}(A_h)^{-1}$. In Figure 5, we plot its smoothing rates in the case $d = 2, p = 4$ with damping parameter $\tau$ ranging from 0.1 to 1.0. Again, the smoother fails to reduce the error in the upper part of the spectrum, regardless of $\tau$.

## 5 Conclusions

We have studied a geometric multigrid method for isogeometric discretizations using a simple model problem. As already observed in [6], V-cycle iteration numbers depend strongly on the spline degree $p$. The local Fourier analysis indicates that even on the real line without boundary conditions, performance degrades as $p$ is increased. CG iteration preconditioned with one V-cycle predictably improves the convergence in the badly performing cases.

The numerical spectral analysis shows that both the Gauss-Seidel and the damped Jacobi smoother fail to reduce high-frequency error components for higher $p$. Higher space dimension compound this problem.

## Acknowledgments

This work was supported by the National Research Network "Geometry + Simulation" (NFN S117, 2012–2016), funded by the Austrian Science Fund (FWF).

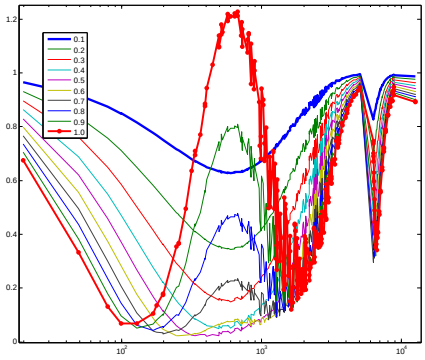


**Fig. 5.** Smoothing factors for the Jacobi smoother ($d = 2, p = 4$) with different damping parameters $\tau$. $x$-axis: $\lambda_j$, $y$-axis: $r^{\mathrm{S}}(\mu_j)$.

The first author was also supported by the project AComIn "Advanced Computing for Innovation", grant 316087, funded by the FP7 Capacity Programme "Research Potential of Convergence Regions".

## References

1. A. Brandt. Rigorous quantitative analysis of multigrid, I: Constant coefficients two-level cycle with $L_2$-norm. *SIAM J. Numer. Anal.*, 31(6):1695–1730, December 1994.
2. A. Buffa, H. Harbrecht, A. Kunoth, and G. Sangalli. BPX-preconditioning for isogeometric analysis. *Computer Methods in Applied Mechanics and Engineering*, 265:63–70, 2013.
3. N. Collier, D. Pardo, L. Dalcin, M. Paszynski, and V. M. Calo. The cost of continuity: A study of the performance of isogeometric finite elements using direct solvers. *Computer Methods in Applied Mechanics and Engineering*, 213–216:353–361, 2012.
4. L. B. da Veiga, D. Cho, L. Pavarino, and S. Scacchi. Overlapping Schwarz methods for isogeometric analysis. *SIAM Journal on Numerical Analysis*, 50(3):1394–1416, 2012.
5. L. B. da Veiga, D. Cho, L. Pavarino, and S. Scacchi. BDDC preconditioners for isogeometric analysis. *Mathematical Models and Methods in Applied Sciences*, 23(6):1099–1142, 2013.
6. K. P. S. Gahalaut, J. K. Kraus, and S. K. Tomar. Multigrid methods for isogeometric discretization. *Computer Methods in Applied Mechanics and Engineering*, 253:413–425, 2013.
7. T. J. R. Hughes, J. A. Cottrell, and Y. Bazilevs. Isogeometric analysis: CAD, finite elements, NURBS, exact geometry and mesh refinement. *Computer Methods in Applied Mechanics and Engineering*, 194(39-41):4135–4195, October 2005.
8. S. K. Kleiss, C. Pechstein, B. Jüttler, and S. Tomar. IETI – Isogeometric tearing and interconnecting. *Computer Methods in Applied Mechanics and Engineering*, 247–248:201–215, 2012.
9. U. Trottenberg, C.W. Oosterlee, and A. Schüller. *Multigrid*. Academic Press, 2001.